Arrhythmogenic Sites Mapping in Post-Ischemic Ventricular Tachycardia Using a Siamese Neural Network

Andrea Pitzus[1], Giulia Baldazzi[1], Luigi Raffo[1], Graziana Viola[2], Danilo Pani[1]

[1]Department of Electrical and Electronic Engineering (DIEE), University of Cagliari, Cagliari, Italy
[2]Clinical and Interventional Cardiology Unit, Santissima Annunziata Hospital, Sassari, Italy

Abstract

Ventricular tachycardia (VT) is a life-threatening arrhythmia commonly treated by catheter ablation guided by substrate mapping. This procedure relies on the cardiologist's visual inspection of intracardiac electrograms (EGMs) to identify arrhythmogenic sites. This task is challenging due to the huge amount of data to interpret.

To address this issue, we proposed a method for discriminating between physiological and anomalous bipolar EGMs based on siamese neural networks (SNN), able to deal with small datasets, for the automatic labeling of the EGMs onto the electroanatomic map.

On a balanced dataset of 1504 physiological and anomalous EGMs, from nine post-ischemic VT patients, we demonstrated that a SNN trained to distinguish between the two types of EGMs is able to achieve a high degree of specificity (91±3%) and sensitivity (93±3%). Potentially, the proposed approach could also be exploited to map the similarity of the EGMs, resulting in a novel electroanatomic map for the identification of areas of abnormal conduction.

1. Introduction

Ventricular tachycardia (VT) is a severe arrhythmia that can cause fainting, loss of consciousness, and even sudden cardiac death. Different treatments for VT have been proposed, including drugs, implantable cardioverter defibrillators, and catheter ablation. The last option is increasingly adopted, because of the advantages with respect to the other two, such as the cost-efficacy ratio and the avoidance of long-term therapies [1].

However, the electroanatomic mapping (EAM) procedure, which is performed to identify arrhythmogenic areas with abnormal conduction, such as areas associated with fractionated and late potentials and/or local abnormal ventricular activities, is time-consuming. Its outcome depends on the expertise of the electrophysiologist, challenged by the huge amount of endocavitary electrograms (EGMs) to be reviewed for the identification of the anomalous ones (AVPs).

Artificial intelligence methods can be deployed to support faster and operator-independent signals interpretation, thus assisting the electrophysiologists during the EAM procedure. To this aim, different artificial intelligence approaches, based on both machine learning [2] and deep learning [3], have been proposed so far. In [3], transfer learning with the AlexNet convolutional neural network (CNN), previously trained on the ImageNet dataset [4], demonstrated a classification accuracy above 90%. There, time-frequency representation by synchrosqueezed wavelet transform (SSWT) [5] was adopted for the creation of the input images.

Siamese neural networks (SNNs) [6] have been shown to be effective in various applications, including cardiac electrophysiology [7], in particular when a limited-size dataset is available. This is because SNNs perform comparisons between instances rather than direct classification, resulting in a significant increase in the number of training and testing examples from N to $N \times (N - 1)/2$. In this work, we investigated for the first time the adoption of a SNN for the identification of AVPs in real bipolar EGMs. Moreover, we explored nonlinear similarity metrics derived from the Siamese model to create a novel EA map aiming at enhancing the presence of AVPs, and as such at identifying arrhythmogenic regions.

2. Materials and methods

2.1. Dataset

All signals adopted in this work were recorded from nine patients with post-ischemic VT (78% male, age: 66 ± 10 years, ejection fraction: 29% ± 6%) during left ventricle EAM procedures carried out at San Francesco Hospital in Nuoro, Italy, performed using CARTO®3 mapping system (Biosense Webster, Inc., Diamond Bar, California).

The bipolar EGMs, sampled at 1 kHz and band-pass filtered between 16 and 500 Hz by the CARTO, were

manually labeled by an expert electrophysiologist using a custom MATLAB graphical user interface [8]. A balanced dataset consisting of 1504 labeled instances, including 752 physiological potentials and 752 AVPs, was used for this work. As previous findings [8] highlighted statistical differences in spectral components between physiological EGMs and AVPs, the input images for the SNN were created by computing three different time-frequency representations of each bipolar EGM, i.e., the continuous wavelet transform (CWT), the Hilbert-Huang transform (HHT) and the SSWT. For each signal, a window of interest of 500 ms around the reference annotation was considered, and then the three transformations were computed and stacked in a 250×250×3 matrix, resulting in a time resolution of 2 ms and a frequency resolution of 2 Hz. This size corresponds to the input layer of the adopted architecture. A detailed representation of the input images is reported in Figure 1.

2.2. Siamese network architecture

To reduce the number of weights to be updated, we designed the SNN architecture adopting a simple subnetwork. The weights of the different layers were initialized by random sampling from a normal distribution with zero mean and standard deviation of 0.01. Each branch of the subnetwork was composed of an input layer (250×250×3), followed by a set of four stacks of three layers, i.e., a convolutional layer (10×10×64, 7×7×128, 4×4×128 and 5×5×256) followed by a ReLu layer, and then by a Max Pool layer (4×4 with stride 4, 3×3 with stride 3, and 2×2 with stride 2), except for the fourth block of the stack, where the last layer was replaced by a fully connected layer with 4096 hidden neurons. Finally, the difference between the subnetworks' outcomes was used as input for the final fully connected layer. A detailed representation of the SNN is reported in Figure 2.

2.3. Training settings

A 10-fold cross-validation approach was adopted to partition the multi-patient dataset of 1504 instances, thus dividing it into 10 balanced folds using the stratified sampling option. In the cross-validation, each partition consisted of eight folds for training and the remaining two for validation and testing, respectively.

Then, to accomplish the task of AVP identification, the network was trained to measure the similarity between two EGMs. To this aim, we assigned the label '1' to the duplet belonging to the same class, '0' otherwise. Indeed, each prediction of the SNN produced a normalized score, which measures the similarity between the two compared instances. Therefore, the SNN was tested by measuring the average similarity between each instance (i.e., EGM) of the test set and the entire set of reference images, including two class-related subsets, i.e., one of the AVPs (50%) and one of the physiological EGMs (50%). Remarkably, to ensure that the network was tested only on previously unseen data, the reference set was chosen identical to the test set but excluding at each time the testing instance. As such, each tested EGM was assigned to the class exhibiting the higher mean similarity.

In this implementation, the binary cross-entropy was selected as the loss function, while we used the stochastic gradient descent with momentum as the training algorithm. The hyperparameters were set according to the typical values adopted in the field, i.e., learning rate equal to 0.001, momentum equal to 0.8, and batch size of 30

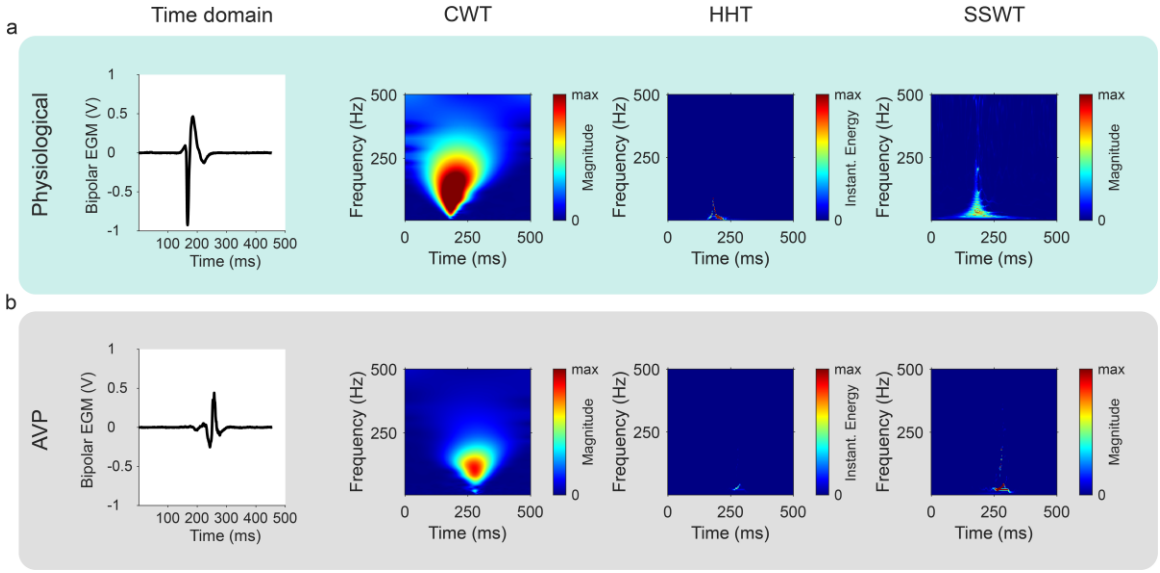

Figure 1: In the top panel (a), different time and time-frequency representations of a physiological EGM are reported, while in the bottom panel (b) different representations of an AVP in time and time-frequency domains are shown.

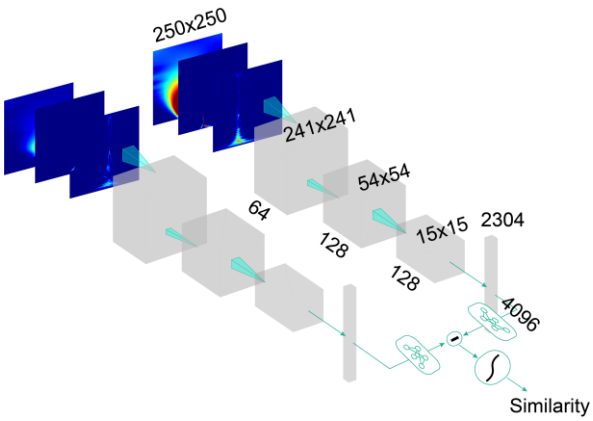

Figure 2: Pipeline for SNN-based AVPs automatic recognition approach proposed in this work, along with a detailed representation of the SNN architecture.

instances per iteration. To avoid overfitting, an early-stop condition was imposed during training, by evaluating the validation set every 50 training iterations, and stopping the training after 30 iterations not decreasing the validation loss.

2.4. Similarity maps

After classification, the EGMs and the corresponding predicted labels were projected onto the EA map, to compare the model outcome with the ground truth provided by the electrophysiologist's annotation. As such, a so-called classification map was obtained, using the voltage map or the local activation time (LAT) map provided by the CARTO as background.

Then to better analyze only the presence of AVPs targeting areas of abnormal conduction, we hypothesized that the AVPs similarity score, previously used to perform the classification, could better highlight at a glance this information into the map. Therefore, a scattered interpolant was used, and the interpolation of similarity values over the map coordinates was performed. Remarkably, not all the points used to compute the CARTO map were included for the AVPs similarity map, since a subsampling was necessary to balance the two classes. Indeed, the regions with a distance greater than 8 mm have been discarded from the map to avoid approximate interpolation. The resulting map is called Similarity map hereinafter. Finally, to give an overview of the variability of the similarity score, we apply the same method previously described but reporting the standard deviation of the variability score.

2.5. Performance evaluation

We evaluated various quantitative indexes to assess the SNN performance, i.e., accuracy (Acc), sensitivity (TPR), specificity (TNR), precision (PPV), and F1 score. While computing such performance indexes, we considered AVPs as positive entries and physiological EGMs as negative entries, thus true positives (TP) counted for all EGMs that were correctly classified as AVPs, false positive (FP) for all EGMs incorrectly classified as AVPs, and true negative (TN) for all EGMs properly recognized as physiological.

3. Results

Table 1 presents the mean and standard deviation of the performance indexes deriving from the 10-fold cross-validation. The results show high discrimination performance, above 91% for all the investigated metrics. Our results revealed a high efficacy of the proposed method in detecting AVPs, even if slightly worse than previous studies adopting a CNN on the same dataset [3]. The lack of pre-training was identified as a plausible explanation of this mismatch, as well as the different input images to the network. However, by considering TPR in Table 1, the detection performance of AVPs was superior when using SNN with respect to AlexNet. Remarkably, this metric is of main importance when the aim is missing any arrhythmogenic site and, possibly, ablation target.

In Figure 3 an example of classification and similarity maps is reported. Both classification maps and the similarity score with the AVPs set showed strong coherence with the EA map provided by the CARTO. Notably, in the similarity map, a conduction pathway without AVPs is highlighted, which was not visible by LAT or voltage maps. Furthermore, as can be seen by low standard deviations of similarity values, the SNN seemed to be confident with its decisions. Therefore, the proposed map could be useful for pinpointing critical endocardial areas with and without AVPs during mapping and ablation procedures.

4. Conclusion

This work proposed the use of SNN for the automatic identification of physiological and anomalous bipolar EGMs in electrophysiological procedures of post-ischemic VT. The results are in line with previous studies exploiting deep learning for the same purpose, but with a higher number of TP, which is encouraging. Moreover, the

Table 1. Mean (μ) and standard deviation (σ) for all metrics computed in the 10-fold cross-validation.

	AlexNet	SNN
Metric	μ±σ	μ±σ
Acc (%)	**92.5±2.5**	91.8±1.7
TPR (%)	92.0±4.0	**92.7±3.4**
TNR (%)	**93.0±3.3**	91.0±3.2
PPV (%)	**93.0±3.0**	91.2±2.8
F1	**0.92±0.03**	0.92±0.02

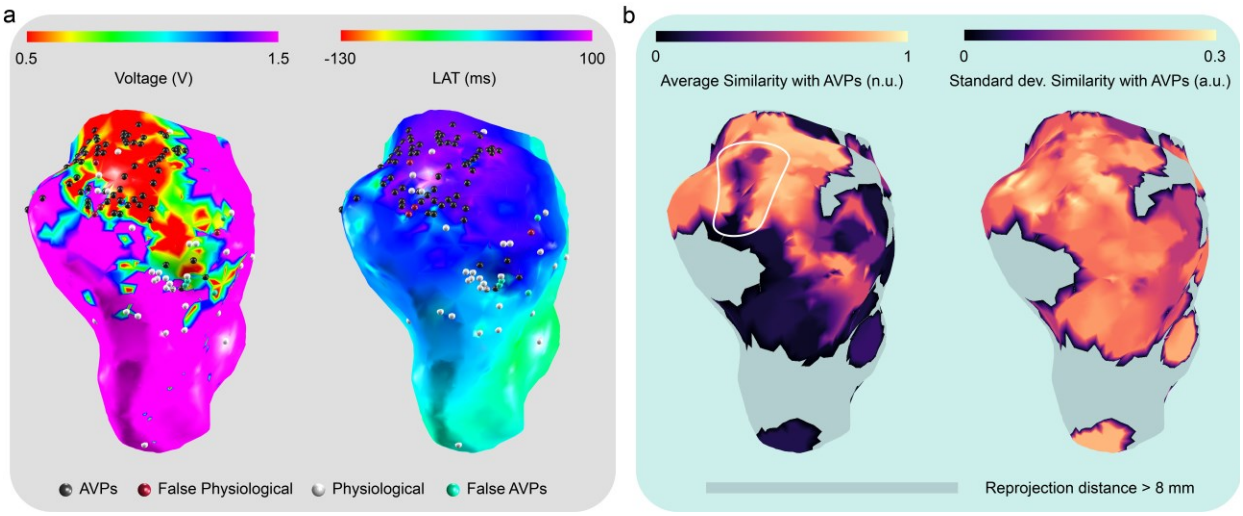

Figure 3: In the left panel, two classification maps are reported with LAT and voltage background, as well as the legend for the tested sites compared to the ground truth provided by the electrophysiologist annotation; in the right panel, (b) the SNN the similarity maps based on average similarity (left) and on its standard deviation (right) are reported. As can be seen, in the average similarity map perspective, a conduction pathway without AVPs is highlighted w.r.t. standard LAT and voltage maps.

previously adopted CNN, i.e., AlexNet, requires more than five times the number of parameters to be updated than the SNN exploited in this work.

Remarkably, we proposed a novel EAM based on the SNN similarity scores, and this map could be further studied to increase the associated information and evaluate its usefulness in the framework of EAM procedures.

Acknowledgments

This work was carried out under the ARGO (Ablation Reinforcement by computer-aided Guidance and Optimization) project, approved by Azienda Tutela Salute Sardegna (ATS Sardegna). The research leading to these results has received funding from the European Union - NextGenerationEU through the Italian Ministry of University and Research under PNRR - M4C2-I1.3 Project PE_00000019 "HEAL ITALIA" to G. Baldazzi, CUP F53C22000750006. The views and opinions expressed are those of the authors only and do not necessarily reflect those of the European Union or the European Commission. Neither the European Union nor the European Commission can be held responsible for them.

References

[1] A. Kanagaratnam et al., "Catheter Ablation for Ventricular Tachycardia in Ischaemic Versus Non-Ischaemic Cardiomyopathy: A Systematic Review and Meta-Analysis," Heart, Lung and Circulation, vol. 31, no. 8, pp. 1064–1074, Aug. 2022, doi: 10.1016/j.hlc.2022.02.014.

[2] G. Baldazzi, M. Orrù, G. Viola, and D. Pani, "Computer-aided detection of arrhythmogenic sites in post-ischemic ventricular tachycardia," Sci Rep, vol. 13, no. 1, p. 6906, Apr. 2023, doi: 10.1038/s41598-023-33866-w.

[3] A. Pitzus et al., "Exploring Transfer Learning for Ventricular Tachycardia Electrophysiology Studies," in 2022 Computing in Cardiology (CinC), Tampere, Finland: IEEE, Sep. 2022, pp. 1–4. doi: 10.22489/CinC.2022.382.

[4] A. Krizhevsky, I. Sutskever, and G. E. Hinton, "ImageNet classification with deep convolutional neural networks," Commun. ACM, vol. 60, no. 6, pp. 84–90, May 2017, doi: 10.1145/3065386.

[5] I. Daubechies, J. Lu, and H.-T. Wu, "Synchrosqueezed wavelet transforms: An empirical mode decomposition-like tool," Applied and Computational Harmonic Analysis, vol. 30, no. 2, pp. 243–261, Mar. 2011, doi: 10.1016/j.acha.2010.08.002.

[6] H. Cartwright, Ed., Artificial Neural Networks, vol. 2190. in Methods in Molecular Biology, vol. 2190. New York, NY: Springer US, 2021. doi: 10.1007/978-1-0716-0826-5.

[7] B. Hunt, E. Kwan, D. Dosdall, R. S. MacLeod, and R. Ranjan, "Siamese Neural Networks for Small Dataset Classification of Electrograms," in 2021 Computing in Cardiology (CinC), Brno, Czech Republic: IEEE, Sep. 2021, pp. 1–4. doi: 10.23919/CinC53138.2021.9662707.

[8] G. Baldazzi, M. Orrù, G. Solinas, M. Matraxia, G. Viola, and D. Pani, "Spectral characterisation of ventricular intracardiac potentials in human post-ischaemic bipolar electrograms," Sci Rep, vol. 12, no. 1, p. 4782, Dec. 2022, doi: 10.1038/s41598-022-08743-7.